Hydrogen bonding and charge transfer: Interaction of OH radical with rare gas atoms

Julie Goodman and L. E. Brus

Citation: The Journal of Chemical Physics **67**, 4858 (1977); doi: 10.1063/1.434665
View online: http://dx.doi.org/10.1063/1.434665
View Table of Contents: http://aip.scitation.org/toc/jcp/67/11
Published by the American Institute of Physics

Hydrogen bonding and charge transfer: Interaction of OH radical with rare gas atoms

Julie Goodman and L. E. Brus

Bell Laboratories, Murray Hill, New Jersey 07974
(Received 1 August 1977)

Hydroxyl radical in solid Ne at 4.2 K is known to rotate freely, vibrationally relax slowly, and have an essentially unperturbed structure. However, the HO structure and dynamics are profoundly affected by solvation in the heavier rare gases Ar, Kr, and Xe. One Ar atom nearest neighbor increases the OH ($A\,^2\Sigma^+$) vibrational relaxation rate by a factor of $\geq 10^3$, and $A\,^2\Sigma^+ \leftrightarrow X\,^2\Pi$ spectra consistant with a linear–linear transition in hydrogen bonded ArHO are observed. The Ar–HO ($A\,^2\Sigma^+$) well depth is $D_0 \approx 675$ cm^{-1} with $\omega_e \approx 203$ cm^{-1} and $\omega_e x_e \approx 13.1$ in solid Ar host; the Kr–HO ($A\,^2\Sigma^+$) well depth is ≥ 1000 cm^{-1}. The Ar–HO hydrogen bond length is shorter by $\Delta r_e = 1.15 \pm 0.1$ Å in the excited state. The OH ($A\,^2\Sigma^+$) (0,0) emission band shifts from 3090 in Ne to 4400 Å in Xe. The theory of hydrogen bond formation in both ground and excited states is discussed, with particular reference to the contribution of charge transfer in various environments. Comparison is made with the spectra of hydrogen halides, and the physical origin of rotation–translation coupling theory is discussed. The role of charge transfer complexes in the gas phase quenching of free radical luminescence by rare gas atoms is also considered.

The present experiments represent an attempt to provide a simple, well characterized prototype for the understanding of electron flow across a hydrogen bond. Specifically we would like to understand how charge transfer contributes to hydrogen bonds, and how hydrogen bonds differ from other weak chemical interactions not involving mediating protons. This relationship between charge transfer and hydrogen bonding is a central issue in continuing theoretical attempts to model hydrogen bonding.[1]

Rare gas atoms are slightly basic (electron donating) and can form weak charge transfer complexes, in the classic spectroscopic sense originally proposed by Mulliken.[2] The strongest diatomic complex appears to be XeF($X\,^2\Sigma$), which has $a \approx 0.15$ eV well depth typical of weak valence interactions.[3] The F atom is isoelectric with the HO radical, and we inquire as to the structure and bonding of XeHO. HO has lower electron affinity (1.82 eV) than the F atom (3.45 eV), and there should be less charge transfer. On the other hand HO ($X\,^2\Pi$) can hydrogen bond and is in fact acidic on both ends: the O atom, because it has a vacant P orbital, can accept charge, and the H atom is naturally acidic. It does not appear possible to predict *a priori* the structure of XeHO. Hydrogen bonding with open shell HO radical thus poses additional questions not found in closed shell alcohol hydrogen bonds.

The lowest excited electronic state in XeF is a charge transfer Xe^+F^- state; in XeHO the $A\,^2\Sigma^+$ valence excited state of HO should occur below the expected Xe^+HO^- states. In XeF the ground state well is spectroscopically rationalized as due to weak mixing between zero order excited Xe^+F^- and ground covalent states. In XeHO, charge transfer bonding character may be mixed into both covalent states correlating with HO ($X\,^2\Pi$) and HO ($A\,^2\Sigma^+$). We attempt to observe these potential surfaces via electronic spectroscopy, in the same way that the ground state well of XeF has been characterized via charge transfer fluorescence.[4]

Previous studies have shown that similar species, such as Kr–HN, have an interaction stronger than van der Waals bonding.[5] In KrHN, the interaction with HN saturates with the first nearest neighbor Kr atom in the solid state, and is not pairwise additive with successive Kr neighbors. This saturation effect appears in both spectral shifts and the vibrational relaxation behavior of the HN stretch. XeHO should be more strongly bound than KrHN because the O atom is more electronegative than the N atom, and Xe is more basic than Kr.

We attempt a systematic study of HO bound to the heavier rare gas atoms R. It is known that minimal interaction exists for NeHO. In solid Ne, HO radical undergoes almost unperturbed free rotation and relatively slow vibrational relaxation.[6,7] The HO and DO ground state vibrational frequencies are within 5 cm^{-1} of their gas phase values. We find that solvation in Ar, however, produces relatively greater structural changes than previously observed for any other small molecule or radical.

The $X\,^2\Pi$ ground state of HO has the MO configuration $\sigma^2\pi^3$. σ is a "bonding" orbital formed by the O atom P_Z and H atom S overlap, while π is formed by the O atom P_Y and P_X orbitals. The $A\,^2\Sigma^+$ excited state is principally $\sigma\pi^4$ in which one "bonding" electron has been promoted to the "nonbonding" π orbital.[8] In polar molecules such as OH, Mulliken[9] has observed that "bonding" and "antibonding" labels are not particularly meaningful. Experimentally it is observed that the permanent dipole increases only slightly from 1.66 to 1.72 ± 0.1 D in $A\,^2\Sigma^+$,[10,11] and that ω_e decreases only slightly from 3735 to 3180 cm^{-1} in $A\,^2\Sigma^+$.

I. EXPERIMENTAL

The apparatus has been previously described.[12] Briefly, we detect time and wavelength resolved resonance fluorescence following pulsed, frequency doubled dye laser excitation of the matrix. The dye laser pulse exhibits $\Delta\lambda \approx 0.05$ Å and $\Delta t \approx 3$–5 nsec.

Isolated HO radicals are obtained by vacuum ultraviolet photolysis of a trace H_2O impurity in the rare gas

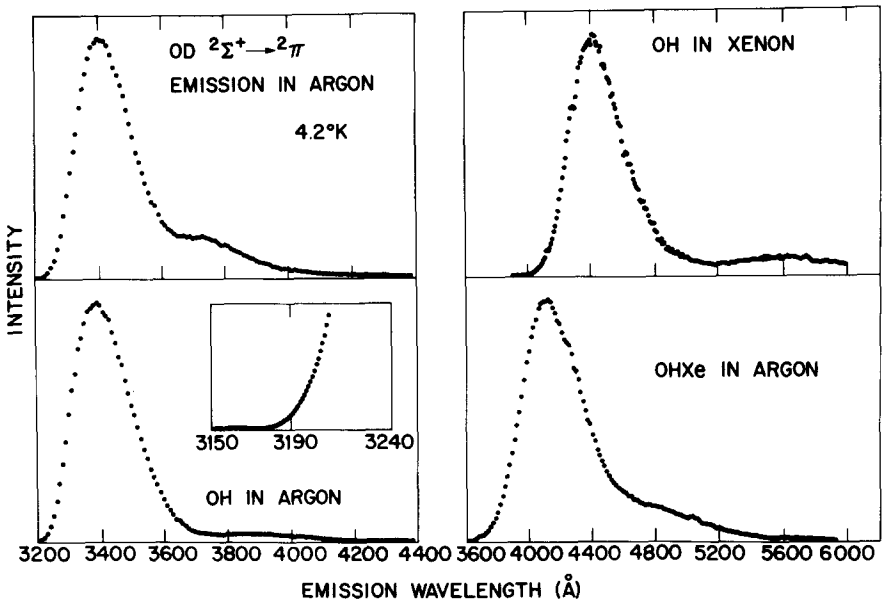

FIG. 1. Digital emission spectra as described in the text. Individual points are 10 Å apart. Insert in lower left hand side gives high resolution spectrum on the blue edge of the OH emission in Ar.

mixtures. The walls of the cryostat and deposition line are passivated with D_2O vapor before DO experiments. The HO in neon[7] and mixed rare gas host[5] techniques have been previously described.

II. OBSERVATION AND DISCUSSION

A. Pure Ar host

If HO in Ar is excited near 2650 Å in the region of the (2, 0) $A\,^2\Sigma^+ - X\,^2\Pi$ absorption, then the broad Fig. 1 (lower left) emission is observed. There is no resolved structure; the maximum is near 3400 Å and has FWHM ≈ 1800 cm^{-1}. The shape is asymmetric with a long tail extending beyond 4000 Å. This emission is totally different from that in a pure Ne host, where sharp rotational structure fluorescence lines occur near 3090 Å.[6,7] The emission observed following excitation of DO(2, 0) in Ar near 2750 Å is similar (Fig. 1, upper left) with the exception of the asymmetric tail, which contracts and becomes a shoulder near 3700 Å. The exponential decay time is $\tau = 475 \pm 10$ nsec without observable rise-time ($\tau_r \leq 20$ nsec) in both cases.

The HO(2, 0), (1, 0), and (0, 0) excitation spectra appear in Fig. 2. The emission spectra and time dependence are experimentally unchanged for excitation anywhere in these regions. In fluorescence, the HO Franck–Condon (hereafter FC) factors strongly favor the $\Delta v = 0$ transitions. The (2, 2) band is shifted by 120 Å from the (0, 0) in the gas phase; our emission shapes are unshifted within a ± 5 Å uncertainty. We conclude that these shapes represent $v' = 0$ emission, and that vibrational relaxation occurs within 20 nsec. In solid neon, the vibrational relaxation rates are several orders of magnitude slower.

Substructure (tabulated in Table I) appears on each (v', 0) band in absorption. This structure, which is totally different than the free rotation structure in a neon host, is an anharmonic six or seven membered progression (v'_σ, 0) in some low frequency mode hereafter labelled ν'_σ. The ν'_σ FC factors for low ν'_σ decrease rapidly, and we have arbitrarily labelled the lowest members as $\nu'_\sigma = 0$. Their extreme weakness makes their location somewhat uncertain.

Comparison of the (2, 0) and (0, 0) substructure indicates that the corresponding ν'_σ ΔG values are somewhat larger for (2, 0), indicating a slightly deeper well. A

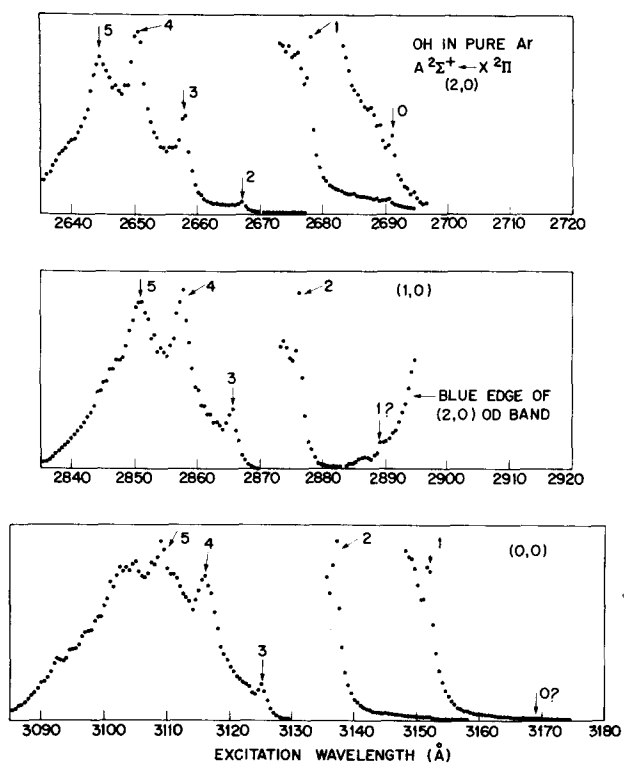

FIG. 2. Digital excitation spectra. Upper, middle, and lower panels give OH(2, 0), (1, 0), and (0, 0) bands in pure Ar. In the (1, 0) case, a slight OD impurity causes rising absorption near 2890 Å. Individual points are 0.5 Å apart. (0, 0) emission at 3400 Å is monitored in all cases.

TABLE I. ν_σ substructure observed in the excitation spectra. ΔG gives the vibrational energy spacing between ν_σ' and $\nu_\sigma' - 1$.

OH in Ar (2,0)				OH in Ar (1,0)				OH in Ar (0,0)			
I	ν_σ'	λ Å	ΔG cm^{-1}	I	ν_σ'	λ Å	ΔG cm^{-1}	I	ν_σ'	λ Å	ΔG cm^{-1}
8	5	2645.3	86	9	5	2851.6	83		5	3109.9	72
10	4	2651.3	103	10	4	2858.3	98		4	3116.9	93
4	3	2658.5	130	4	3	2866.3	127		3	3125.9	122
0.6	2	2667.8	154	0.4	2	2876.8	156		2	3137.9	154
0.06	1	2678.8	180		1	2889.8			1	3153.1	168
0.006	0	2691.8			0				0	~3169.9	
OD in Ar (2,0)				OD in Ar (1,0)				OH in Kr (2,0)			
10	5	2742.8	80	6	6	2902	68	9	7	2654.5	96
8	4	2748.8	99	10	5	2907.5	83	10	6	2661.3	95
2	3	2756.3	124	5	4	~2915	110	8	5	2668	105
~0.2	2	2765.8	163	0.5	3	~2924		5	4	2675.5	139
~0.01	1	2778.3						3.5	3	2685.5	152
	0							2	2	2696.5	178
								1	1	~2709.5	215
								~0.4	0	~2725	

linear Birge–Sponer extrapolation for $v' = 2$ yields $D_0 = 755$ cm^{-1}, while $D_0 = 675$ cm^{-1} for $v' = 0$. Approximate Morse oscillator parameters for $v' = 2$ are $\omega_\sigma = 202$ cm^{-1} and $\omega x_\sigma = 12.6$ cm^{-1}, while those for $v' = 0$ are $\omega_\sigma = 203$ cm^{-1} and $\omega x_\sigma = 13.1$ cm^{-1}. The HO ($A\,^2\Sigma^+$) vibrational constants can be obtained from the ν_σ' (1, 0) locations which have been measured for all three v' states. We find $\Delta G_{1/2} = 2890$ cm^{-1} and $\Delta G_{3/2} = 2726$ cm^{-1}; in the free radical in vacuum, these numbers are 2987 cm^{-1} and 2793 cm^{-1}, respectively. We see there is a distinct change in $A\,^2\Sigma^+$ potential curve shape upon solvation in Ar at 4.2 K.

Figure 3 and Table I also exhibit the observed substructure for DO. The isotopic change in corresponding ν_σ' ΔG value is small and on the order of ~5%; individual values are somewhat uncertain because of inaccuracy in measuring maxima of these somewhat broad bands. The data are not consistent with the $\sqrt{2}$ isotope effect expected if ν_σ' represented a proton motion.

B. ArHO in neon host

In order to understand the interaction between HO and the host, and to identify ν_σ', it is useful to compare HO in pure Ar and pure Ne gas hosts with HO that has one Ar nearest neighbor and is otherwise surrounded by neon. This sort of experiment was previously carried out in an attempt to understand the vibrational relaxation mechanism of HN.[5] We observe two types of fluorescing HO species (HO "sites") in matrices where the host is a 0.5 to 3.0% solution of Ar in Ne. The dominant site is "neon-like" in that the time dependent and spectra data are the same as those in pure Ne. "Neon-like" sites are interpreted as those with all neon nearest neighbors.

The minor site is "argon-like" in most (but not all) of its properties. Vibrationally relaxed emission, with emission spectra *identical* to those in Fig. 1. occur for both HO and DO. The observed lifetimes lengthen, with a value $\tau = 690$ nsec observed for HO in a 0.5% Ar in Ne matrix. This value is longer than the 582 nsec value in pure Ne and the 475 nsec value in pure Ar. The excitation spectra show resolved (v', 0) bands, but the ν_σ' substructure observed in pure Ar is not present. Figure 3 compares the DO (2, 0) excitation spectra in pure Ar with that of the "argon-like site." Besides the loss in substructure, the "argon-like" site (2, 0) band shows a slight blue shift. The "argon-like" site is interpreted as HO (DO) with one Ar nearest neighbor.

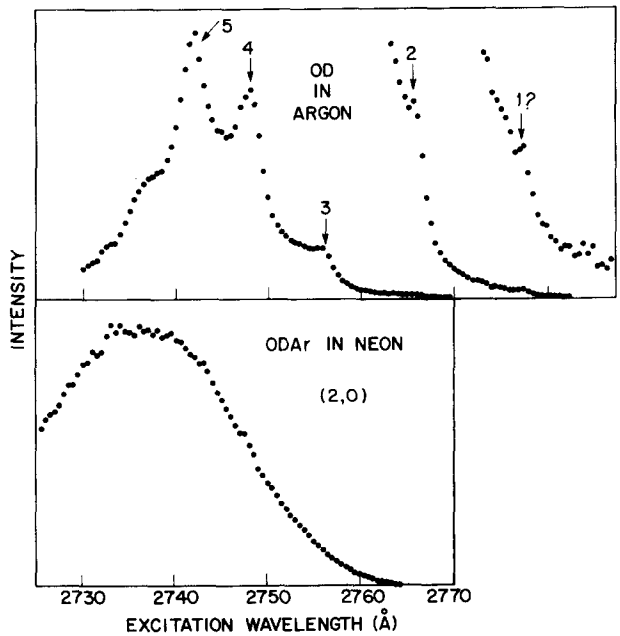

FIG. 3. Digital excitation spectra of OD (0, 0) emission at 3400 Å as in Fig. 2.

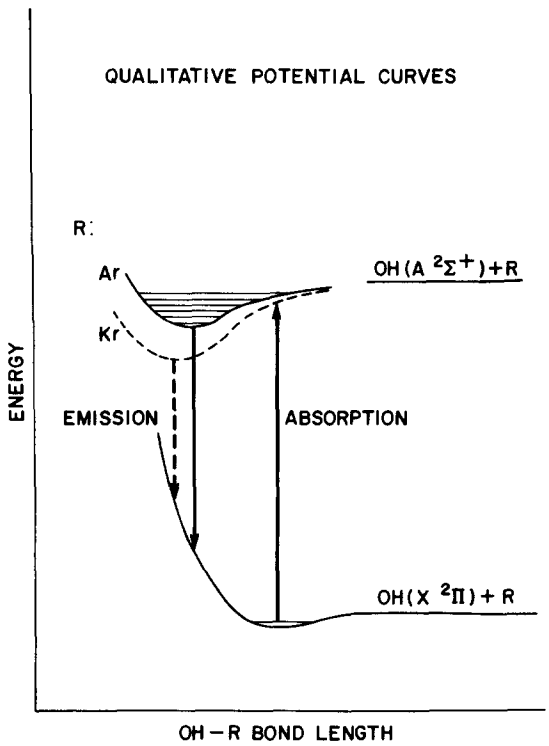

FIG. 4. Qualitative potential energy curves for absorption and vibrationally relaxed emission as a function of the hydrogen bond length. Solid curve is R = Ar, while dotted curve is R = Kr. The figure does not show an expected smaller change in ground state curves between Kr and Ar.

In pure Ne the OD($A\,^2\Sigma^+$) vibrational relaxation rate k is 4×10^4 sec^{-1}. In pure Ar, the rate is too fast to time resolve and we conclude $k \geq 5\times10^7$ sec^{-1}. The "argon-like" site data shows us that an (at least) 3 orders of magnitude increase in rate occurs with only one Ar nearest neighbor. This result is consistent with the HN experiments, in which the increase in k from pure Ar to pure Kr was reproduced by just one Kr nearest neighbor.[5] Moreover the pure Ne free rotation fine structure in both absorption and emission is eliminated by just one Ar nearest neighbor. The broad $v' = 0$ emission spectrum shape is unchanged by addition of further Ar nearest neighbors, and therefore must be interpreted in terms of the internal structure of a triatomic molecule ArHO.

In pure neon, the $v' = 0$ levels were concluded to have fluorescence quantum yields of nearly 1.0. The transition dipole is essentially unchanged from its gas phase value. The shortening of the radiative lifetime from 788 ± 13 nsec in vacuum to 582 ± 10 nsec in neon principally represents an increase in the radiation field density of states in a medium with index of refraction greater than 1.[7] In pure Ar and in the "argon-like" site in pure neon, the equality of the HO and DO lifetimes implies that the fluorescence quantum yields are again nearly 1.0. The $v' = 0$ levels remain purely radiative as the solvent interaction increases, apparently because the only possible radiationless transition, internal conversion in $X\,^2\Pi$, is slow due to very low FC factors. In the case of a 0.5% Ar in Ne matrix, we would expect the influence of host index of refraction on the radiative lifetime to be essentially unchanged from pure neon. The observed HO lifetime lengthening from HO in neon to ArHO in neon is roughly consistent with the expected ν^{-3} dependence of τ upon (0, 0) emission frequency ν.

The principal difference between ArHO in neon and HO in pure Ar is the absence of substructure in the excitation spectra. Let us begin to understand this difference in terms of a linear–linear transition of the triatomic molecule ArHO. The underlying idea here is that HO is hydrogen bonded to one Ar atom in both excited and ground electronic states. Independent justification for this model is discussed in a subsequent section.

The high frequency and low frequency stretches of ArHO could be active in a linear–linear transition. The deuterium isotope effect is consistent with the low frequency ν_σ' mode (observed in pure Ar) being the Ar–HO stretch. As shown in Fig. 4, if the hydrogen bond contracts in the excited state then bound structure appears in absorption. However, the subsequent relaxed fluorescence is a photodissociation continuum principally populating unbound levels above the Ar–HO ground state dissociation limit. The fact that the emission continuum (Fig. 1) occurs for both ArHO in neon and for HO in pure Ar implies that this shape should be interpreted only in terms of the internal vibrations of ArHO.

Why does this photodissociation continuum have an isotopically dependent, asymmetric tail? We assign the main band at 3400 Å to (0, 0) fluorescence in both isotopes. The long wavelength tails in both spectra have the correct positions to be (0, 1) emission bands. In gas phase HO, the (0, 1) band intensity is only 0.016 of the (0, 0) intensity.[13] In ArOH the (0, 1) band (Fig. 1(a)) has a higher relative strength, and we conclude that the FC factors have changed in ArHO. This change is further evidence for a "strong" interaction between HO and the Ar atom. Note also that the (0, 1) ArHO band has a wider FWHM than the (0, 0). This implies that the Fig. 4 potential energy curves for motion along the OH–Ar stretch are a sensitive function of the HO internal vibrational state.

Individual ArHO vibronic absorption bands, in principal, have superimposed homogeneous and inhomogeneous line shapes. The homogeneous line shape is the phonon contour plus any possible lifetime broadening. Inspection of Fig. 2 shows that the widths of the $(v_\sigma', 0)$ peaks increase at higher v_σ'. These peaks appear to be ZPL (zero phonon lines) that are lifetime broadened at higher v_σ' where the ΔG values become small. Extremely fast relaxation is expected as ΔG approaches the ≈ 50 cm^{-1} size of a host lattice phonon. A given $(v_\sigma', 0)$ ZPL rests on the "red tail" of the $(v_\sigma' + 1, 0)$ ZPL. This red tail is probably due to both inhomogeneous and lifetime broadening. For low v_σ' the FC factors decrease so rapidly that a $(v_\sigma, 0)$ ZPL is a small bump on the "red tail" of $(v_\sigma + 1, 0)$.

The loss of ArHO vibronic structure upon going from Ar host to Ne host is consistent with a ≈ 50 cm^{-1} increase in linewidth, due either to inhomogeneous broad-

ening or development of a stronger phonon wing. An increase in the homogeneous linewidth from Ar host to Ne host has been observed for the similar species XeO.[14] The (2, 0) ArDO peak in Ne host is slightly blue shifted with respect to Ar host; this observation is consistent with an increased phonon wing in Ne host. A 50 cm^{-1} increase in linewidth is sufficient to blur structure in absorption; in emission this increase is insignificant with respect to the intrinsic ≈ 1800 cm^{-1} (0, 0) width. No detectable change in emission spectra is observed.

Thus the principal distinction between ArOH in Ne and in Ar hosts seems to be a linewidth increase in Ne. The conversion of the Ne host free rotation spectra to vibronic spectra consistent with Fig. 4, and a $\geq 10^3$ increase in vibrational relaxation rate, appear to be properties of ArHO ($A\,^2\Sigma^+$) that are not further affected by additional nearest neighbor Ar atoms. These results are consistent with our previously proposed model for diatomic (HO) vibrational relaxation in solid host.[5] This model proposes internal vibrational energy redistribution in a triatomic complex (ArHO) as the rate limiting step.

In Table I it is assumed that the lowest observed absorption band at 31 547 cm^{-1} in pure Ar is the ν_σ' (0, 0) for HO ($A\,^2\Sigma^+, v' = 0$). The resulting fluorescence from $v_\sigma' = 0$ and $v' = 0$ of ArHO can be observed with available signal to noise as far blue as ≈ 3180 Å (31 446 cm^{-1}). This value is a lower limit for the true ν_σ' (0, 0) energy. The extrapolated position of the next possible lower absorption band is $\approx 31\,350$ cm^{-1}, which lies below our lower limit. This result is strong evidence that the Table I assignments, and the ω_σ and $\omega_\sigma x_\sigma$ values previously given for Ar–HO, are correct. This result also implies that the extreme blue edge of the fluorescence probably populates bound levels of the ground state AR–HO ($X\,^2\Pi$) potential well. The ground state well will subsequently be shown to be much shallower, and the putative substructure features are therefore closer together and more severely lifetime broadened. The resulting fluorescence appears continuous.

C. Pure Kr host

The observations are generally similar to those of pure Ar. The excitation spectra show a less well resolved substructure that is tabulated in Table I. The ν_σ' (v_σ', 0) bands exhibit a milder fall off in FC factors for low v_σ' than in pure Ar. For HO ($A\,^2\Sigma^+, v' = 2$) a total of eight bands are observed, while only six occur in Ar. If the lowest band is actually $v_\sigma' = 0$, then $\omega_\sigma = 235$ cm^{-1} and $\omega x_\sigma = 12.4$ cm^{-1} with $D_0 = 1000$ cm^{-1} via a linear Birge–Sponer extrapolation. This D_0 value should be considered a lower limit. In fluorescence, there is a large shift in the (0, 0) FC maximum from 3400 Å in Ar to 3630 Å in Kr. As in Ar, the emission spectra are vibrationally relaxed. The lifetimes are 450 ± 20 nsec, independent of isotope.

These observations suggest that in KrHO the excited state hydrogen bond is stronger and has a shorter r_e' (relative to the ground state) than in ArHO. In Fig. 4 a deeper well is consistent with the ν_σ' substructure analysis and the milder fall off in ν_σ' FC factors. The red-shifted (0, 0) fluorescence FC maximum appears to principally reflect a greater $r_e' - r_e''$ in KrHO, and secondarily a red shift in the $v' = 0$ and $v_\sigma' = 0$ energy in Kr with respect to Ar.

D. Pure xenon and XeHO in neon host

The trends observed in Kr host are strongly pronounced in Xe host. As shown in Fig. 1 the (0, 0) FC fluorescence maximum shifts to 4400 Å. In absorption the (v', 0) bands are broadened and show no resolvable substructure. The measured lifetime is 100 ± 4 nsec for OH. There are distinct differences between pure Xe and XeHO in neon host. In the latter case, the (0, 0) FC maximum shifts only to 4100 Å, and the measured lifetime is 450 ± 30 nsec. However, no resolvable substructure appears in absorption as in the case of pure Xe.

These results for XeHO emphasize an intrinsic limitation of electronic spectroscopy in matrices: limited information is obtained if internal spectral structure is "blurred" by coupling to host phonon modes.

III. THEORY

A. Hydrogen bonding and charge transfer

Our data are consistent with linear ArHO structures in both excited and ground electronic states. What geometries are theoretically expected? If the bonding were entirely due to charge transfer, then the complex reflects e^- donation by Ar into the lowest unoccupied orbital of HO. The $A\,^2\Sigma^+$ ($\sigma\pi^4$) state has a half full σ "bonding" orbital, and thus in the $A\,^2\Sigma^+$ state we might expect a linear ArHO structure with donation into this "bonding" orbital. For $A\,^2\Sigma^+$ the hydrogen bonding and charge transfer complex geometries are the same. We observe that the ω_e of HO decreases in the ArHO ($A\,^2\Sigma^+$) molecule with respect to the free HO value. This decrease is typical of normal hydrogen bonded complexes. However, in the charge transfer picture we might have expected an increase in ω_e as charge is donated into a nominally "bonding" orbital.

In the ground $X\,^2\Pi$ ($\sigma^2\pi^3$) state, the charge transfer geometry allowing greatest overlap with the empty P orbital on O atom is a 90° bent ArHO structure with O in the center. However, longer range charge transfer may still contribute to the stability of the hydrogen bonded, linear ArHO structure, via admixture of a small component of linear $^2\Pi$ charge transfer Ar^+HO^- state in which π charge is transferred from a P orbital of Ar to the empty orbital of the O atom.[15]

Two separate arguments suggest that the correct ground state geometry is linear ArHO. Firstly, Acquista *et al.*[16] found that the $\Delta G_{1/2}$ vibrational spacing of OH ($X\,^2\Pi$) in solid Ar is red shifted ≈ 130 cm^{-1} from its gas phase value. Table II indicates that this shift, which is a classical indication of moderate hydrogen bonding, is more than an order of magnitude larger than is normally observed for covalently bonded small molecules and radicals in rare gas solids. In the 90° bent ArOH geometry, there would be a slight tendency of ω_e to move towards its value in HO^- ($\sigma^2\pi^4$) ion. ω_e for HO^-

TABLE II. Vibrational spacings and gas to solid spectral shifts for common small molecules. The HCl and H_2O data appear to indicate a tendency towards weaker hydrogen bond formation.

Species	Host	$\Delta G_{1/2}$ cm^{-1}	Shift cm^{-1}	Ref.
$HO(X^2\Pi)$	Ne	3573	+3	6
$HO(X^2\Pi)$	Ar	3452.3	−118	16
		3428.2	−142	
$HN(X^2\Sigma^-)$	Ar	3131	+5	25
$H_2O(\nu_1)$	N_2	3632.5	−19.2	a
$HCl(X^1\Sigma)$	Ar	2885.5	−15.1	b
$CN(X^2\Sigma^+)$	Ne	2043.2	+1	c
$CO(X^1\Sigma)$	Ar	2138.6	−4.9	d
$O_2(X^3\Sigma_g^-)$	N_2	1553.8	−2.4	e
$NO(X^2\Pi)$	Ar	1873.7	−2	f
$ICl(X^1\Sigma)$	Ar	376.4	−5	g
$Cl_2(X^1\Sigma)$	Ar	549.2	−5.1	h

[a]A. J. Tursi and E. R. Nixon, J. Chem. Phys. **52**, 1528 (1970).
[b]A. J. Barnes, in *Vibrational Spectroscopy of Trapped Species*, edited by H. E. Hallam (Wiley, New York, 1973), Table 4.5.
[c]V. E. Bondybey, J. Chem. Phys. **65**, 2296 (1965).
[d]D. Dubost, Chem. Phys. **12**, 139 (1976).
[e]Julie Goodman and L. E. Brus, J. Chem Phys. **67**, 1482 (1977).
[f]R. P. Frosch and G. W. Robinson, J. Chem. Phys. **41**, 367 (1964).
[g]V. E. Bondybey and L. E. Brus, J. Chem. Phys. **64**, 3724 (1976).
[h]V. E. Bondybey and C. Fletcher, J. Chem. Phys. **64**, 3617 (1976).

appears to be larger than ω_e (HO) by a small amount (0–85 cm^{-1}),[17] and thus the experimental $\Delta G_{1/2}$ in pure Ar does not appear consistent with a bent ROH charge transfer structure.

Secondly, our electronic absorption data show a single low frequency progression. The isotopic data prove this mode is not the bending mode of ArHO. If only the Ar–HO stretch appears in the spectrum, then the electronic transition occurs without change in the triatomic bending angle. If one accepts on theoretical grounds that the excited state is linear, then the ground state is also linear.

In summary, the decrease in ω_e in the excited $A^2\Sigma^+$ state, and the apparent linear geometry of ground state ArHO ($X^2\Pi$), suggest that the interaction between open shell HO and the Ar atom is more than a simple weak charge transfer. The ArHO system is sufficiently small that it would appear to be a good candidate for a detailed numerical molecular orbital investigation of the various contributions to the total interaction. The ground state structure with a H atom in the center is consistent with Walsh's rules for covalently bonded triatomic molecules, which normally predict the most electropositive atom in the center. Klemperer and co-workers have previously noted the utility of Walsh's rules in other weakly bonded complexes.[18]

Further evidence that a substantial change in structure upon solvation in Ar requires more than simply a high net electron affinity is provided by the CN radical, which has an electron affinity of 3.82 eV. This value is 2.0 eV higher than that of HO, yet the ω_e in solid Ar is within 4 cm^{-1} of its gas phase value.[19]

It is worthwhile to compare the 11 electron system NeHO ($X^2\Pi$) with the 12 electron system NeHF ($X^1\Sigma$), whose stability Herzberg has discussed using MO arguments.[20] In NeHF there are eight π electrons which fill slightly bonding and antibonding π orbitals formed from P_X and P_Y functions on both Ne and F. These filled orbitals contribute no net bonding, and the stability of NeHF results from σ orbital interaction with a low lying ionic excited state of HF. In NeHO, there are only three electrons in the antibonding π orbital; the π system now also contributes stability in addition to the σ system. The net effect of removing one antibonding electron is a small net transfer of π charge from Ne to O, as discussed above. The neon complexes are undoubtedly both very weakly bound. We might speculate, however, that ArHO ($X^2\Pi$) is actually more strongly bound than ArHF.

The systematic behavior of the RHO spectra as a function of rare gas R, and the variations in different hosts, can be understood using Mulliken's charge transfer arguments.[2] The interaction strengthens as the charge transfer contribution to the hydrogen bond increases. The linear excited transfer state R^+HO^- has both $^2\Sigma$ and $^2\Pi$ molecular components which may individually interact with the lower covalent $X^2\Pi$ and $A^2\Sigma^+$ "hydrogen bond" RHO states. The mixing, in principal, varies as ΔE^{-2}, where ΔE is the energy difference between lower covalent and higher ionic states. As the R^+HO^- states move to lower energy with heavier R, greater percent decreases in ΔE occur for excited $A^2\Sigma^+$ than ground $X^2\Pi$. Therefore the excited state well preferentially deepens in the heavier R cases.

The strong difference between NeHO and ArHO reflects the fact that the ionization potential of Ne is 5.8 eV higher than that of Ar. The solvent, as well as R, will also affect ΔE. The solvent preferentially stabilizes ionic states with respect to covalent states, as shown in the case of XeF where excited charge transfer states have been directly observed.[3] In an Ar host this Xe^+F^- red shift was 0.31–0.47 eV; larger stabilizations should occur in the heavier rare gases. A related phenomenon is the decrease in the solvated R atom ionization potential. For example, the Xe atom ionization potential is 12.13 eV in vacuum, 10.5 eV in solid Ar, and 9.28 eV in pure xenon.[21]

It is perhaps worthwhile to attempt relatively simple estimates of R^+HO^- energies. The difference between the ionization potential of Ar and the electron affinity of HO is 13.9 eV in vacuum. If we assume a distance of 3.54 Å between Ar and O in linear Ar^+HO^-, then the Coulomb attraction lowers the Ar^+HO^- state energy to 10.0 eV above ArHO $X^2\Pi$.[22] This distance 3.54 Å is chosen as it is the Ar–F distance in ArHF.[23] The ΔE values are large, and should not be strongly affected by solvation of ArHO in Ne or in Ar as experimentally observed. However, the Xe^+HO^- energy in vacuum is 7.0 eV; we have allowed for the increased van der Waals diameter of Xe by taking a charge separation of 4.1 Å. In vacuum, ΔE for $A^2\Sigma^+$ is 2.9 eV in XeHO; ΔE will be strongly affected if the Xe^+HO^- energy is lowered by 1 eV or more by solvation in solid Xe. A substantial decrease in ΔE by solvation in solid Xe is consistent with

the observed shift in the (0, 0) FC maximum from 4100 Å for XeHO in Ne to 4400 Å for XeHO in Xe. These estimates simply serve to rationalize the observed trends, and should not be taken literally.

B. Ground state of ArHO in Ar host

Qualitative potential energy curves appear in Fig. 4. The excited state for $v' = 2$ is approximately represented by a Morse potential with $\omega_e \approx 202$ cm^{-1} and $\omega_e x_e = 12.6$ cm^{-1}. Some information concerning the ground state can be obtained by fitting the ν_σ' substructure FC factors in Table II. We represent the lower level as a harmonic oscillator $v_\sigma'' = 0$ wavefunction, and numerically calculate FC factors with upper level Morse oscillator wavefunctions. The best fit is obtained with $\Delta r_e = 1.15 \pm 0.1$ Å and $\omega_e' = 40 \pm 15$ cm^{-1}. We see that in the excited ArHO ($A\,^2\Sigma^+$) state the hydrogen bond length is much shorter, and the well depth is apparently much larger. These results suggest that the ground ArHO ($X\,^2\Pi$) state is considerably closer to the van der Waals limit. Recall, however, that the infrared results indicate a substantial OH ω_e change with no evidence for free rotation.

C. Physical origin of rotation-translation coupling theory, and comparison with other diatomic hydrides

The observed small deviations from free rotation by ground state hydrogen halides HX in rare gas lattices have been explained by a model coupling the HX "center of mass oscillation" with HX rotation via first order perturbation theory.[24] Simple splitting of free rotor levels by an anisotropic host potential does not reproduce the observed spectra.

The RT model postulates that HX is confined inside a "cage" by rigidly fixed host atoms. The cage is mathematically represented by an external potential applied to the HX "center of interaction," which is a point (determined by the electronic wavefunction) that is not necessarily coincident with the HX center of mass. A fundamental assumption is that the host atom locations are determined by the "rigid" structure of the host in the absence of the guest.

We suggest the following modifications, which incorporate (a) the hydrogen bonding tendency of HN, HO, and HX molecules, and (b) the elastic, easily deformable nature of rare gas crystals.[25] Consider an undistorted O_h vacancy. If HX is inserted inside the vacancy but not allowed to rotate, we suggest that HX bonds to one R atom with a triatomic structure similar to that of free RHX.[26] The "center of mass" oscillation of RT theory is principally ν_σ' of triatomic RHX. Other nearby R atoms distort their initial O_h positions in order to effectively solvate RHX.

The lowest librational level of RHX is 12-fold degenerate as HX could initially bond to any nearest neighbor R. The barrier against tunneling from one minimum to the next is controlled by (a) the ν_2 bending potential of free RHX, and (b) the extent of solvation about RHX. If HX does tunnel to a new minimum, the R atom distortion must reorganize about the new axis. The tunneling HX moiety is mathematically rotating about the center of the undistorted vacancy, which almost certainly is not coincident with the HX moiety center of mass. The different equivalent orientations of the RHX axis in space fixed coordinates is given by the O_h symmetry of the undistorted vacancy, while at no specific instant do the nearest neighbor nuclei describe O_h symmetry. In the limit of weak bonding, such that all twelve R atoms have equal order of magnitude interaction energies with HX, the RT model is more nearly correct. Nearly free rotation occurs.

ArHO ($A\,^2\Sigma^+$) corresponds to the opposite limit of strong bonding. ν_σ' of ArHO ($A\,^2\Sigma^+$) is much larger than possible splittings of the substructure bands due to tunneling between equivalent minima. Such small tunneling splittings, which in principal must be present in our spectra, are covered up by various broadening processes. HO ($A\,^2\Sigma^+$) passes from the weak bonding to strong bonding limit between Ne and Ar hosts. However, HN ($A\,^3\Pi$) still tends toward the weak limit in the Ar host, in the sense that the spectra show tunneling structure with no evidence for an absorption progression in ν_σ'.[27] The stronger hydrogen bond in ArHO is consistent with the greater electronegativity of the O atom. The NH ($A\,^3\Pi$) spectra in Ar implied that the positions of minimum potential energy corresponded to HN pointing at Ar atoms, and not at interstitial holes.[27] In retrospect this result reflects a tendency towards linear ArHN complexes.[28]

D. Gas phase quenching of free radical emission by rare gas atoms

Normally rare gas atoms quench molecular and atomic excited states with cross sections σ many orders of magnitude below gas kinetic. The qualitative reason is that there is only a weak van der Waals interaction. However, our discussion of the importance of charge transfer in ArHO indicates that this generalization breaks down if an excited state with high electron affinity collides with one of the heavier rare gases. There may be a correlation between electron affinity and σ. Such a correlation should only be semiquantitative as other properties such as free radical interval level structure and hydrogen bonding ability, also should influence σ.

The excited ArHO complex at 4.2 °K is purely radiative; the gas phase Ar atom σ for OH ($A\,^2\Sigma^+$) is only 0.047 Å^2.[29] The FC factors for OH ($A\,^2\Sigma^+$) internal conversion into HO ($X\,^2\Pi$) are small and apparently hinder both processes. We suggest that σ for Xe atom, which apparently has not been measured, will be much higher.

O (^1D) has an electron affinity of 3.7 eV. The Xe atom actually quenches O (^1D) to O (^3P) with a σ about 0.4 of the gas kinetic cross section.[30,31] The high polarizability of Xe is not involved, as more polarizable SF_6 has an unmeasurably small σ for O (^1D). In this case it is known that an Xe–O (^1D) attractive well of ~0.7 eV exists, and there are favorable diatomic FC factors due to a curve crossing.[14]

CN ($B\,^2\Sigma^+$) has an electron affinity of 7.0 eV.[32] Bersohn and co-workers[33] measured a 3 Å^2 quenching cross

section for Xe atom, and concluded that this very strong interaction was "chemical" and also not related to the Xe atom polarizability. Our charge transfer complex discussion provides a specific spectroscopic model for this system. In CN, FC factors are relatively high for $B^2\Sigma^+ \rightarrow A^2\Pi$ crossing. Finally, note that C_2 radical has a ground state electron affinity ≈ 3.5 eV.[34] The various C_2 excited electronic states will have electron affinities higher by their various T_e values, and strong quenching by Xe is expected.

In the HO, CN, and C_2 cases, one might search for the bound→bound electronic absorption spectra of the charge transfer complexes in a conventional flash photolysis experiment. The ground state complex should be formed by three body collisions of the free radical in a high pressure rare gas.

[1]P. A. Kollman and L. C. Allen, Chem. Rev. **72**, 283 (1972).
[2]R. S. Mulliken, J. Am. Chem. Soc. **64**, 811 (1952).
[3]Julie Goodman and L. E. Brus, J. Chem. Phys. **65**, 3080 (1976).
[4]J. Tellinghuisen, G. C. Tisone, J. M. Hoffman, and A. K. Hays, J. Chem. Phys. **64**, 4796 (1976).
[5]J. Goodman and L. E. Brus, J. Chem. Phys. **65**, 3146 (1976).
[6]D. S. Tinti, J. Chem. Phys. **48**, 1459 (1968).
[7]L. E. Brus and V. E. Bondybey, J. Chem. Phys. **63**, 786 (1975).
[8]S. I. Chu, M. Yoshimine, and B. Liu, J. Chem. Phys. **61**, 5389 (1974).
[9]R. S. Mulliken, Phys. Rev. **50**, 1017 (1936).
[10]F. X. Powell and D. R. Lide, J. Chem. Phys. **42**, 4201 (1964).
[11]E. M. Weinstock and R. N. Zare, J. Chem. Phys. **58**, 4319 (1973).
[12]J. Goodman and L. E. Brus, J. Chem. Phys. **65**, 1156 (1976).
[13]R. W. Nicholls, Proc. Phys. Soc. London Sect. A **69**, 714 (1956).
[14]Julie Goodman, J. C. Tully, V. E. Bondybey, and L. E. Brus, J. Chem. Phys. **66**, 4802 (1977).
[15]It may be that, if the linear Ar^+HO^- state were formed in a vertical transition, it would then spontaneously rotate into the bent Ar^+O^-H structure.
[16]N. Acquista, L. J. Schoen, and D. R. Lide, Jr., J. Chem. Phys. **48**, 1534 (1968).
[17]H. Hotop, T. A. Patterson, and W. C. Lineberger, J. Chem. Phys. **60**, 1806 (1974).
[18]S. J. Harris, S. E. Novick, W. Klemperer, and W. E. Falconer, J. Chem. Phys. **61**, 193 (1974).
[19]D. E. Milligan and M. E. Jacox, J. Chem. Phys. **47**, 278 (1963).
[20]G. Herzberg, *Electronic Structure of Polyatomic Molecules* (Van Nostrand, Princeton, 1967), p. 424.
[21]J. Jortner, *Vacuum Ultraviolet Radiation Physics*, edited by E. E. Koch (Pergamon, New York, 1976), p. 263, Table 12.
[22]We are considering here the Ar^+HO^- energy for a vertical transition from the linear ground state ArHO ($X^2\Pi$) structure. If the charge transfer state actually has a bent R^+O^-H equilibrium geometry, then charge transfer bands in the vuv would be very broad and diffuse.
[23]S. J. Harris, S. E. Novick, and W. Klemperer, J. Chem. Phys. **60**, 3208 (1974).
[24]H. Friedman and S. Kimel, J. Chem. Phys. **43**, 3925 (1965).
[25]L. E. Brus and V. E. Bondybey, J. Chem. Phys. **65**, 71 (1976).
[26]Our solvation results suggest that RHX would be somewhat more strongly bound in the solid than in vacuum. It would be instructive to know the size of ν_0', and its reduced mass, for a ArHX triatomic in vacuum, in Ne, in Ar, and in Xe solid hosts.
[27]V. E. Bondybey and L. E. Brus, J. Chem. Phys. **63**, 794 (1975).
[28]Note that usually fluorescence depolarization is a more sensitive test for tunneling between minima than is spectral structure. Resolvable tunneling splittings of a few cm^{-1} correspond to picosecond tunneling rates, while fluorescence depolarization is measured on the much longer 10^{-9}–10^{-3} time scales of normal excited states.
[29]P. Hogan and D. D. Davis, J. Chem. Phys. **62**, 4574 (1975).
[30]R. J. Donovan, L. J. Kirsch and D. Husain, Trans. Faraday Soc. **66**, 774 (1969).
[31]L. E. Brus and M. C. Lin, J. Phys. Chem. **76**, 1429 (1972).
[32]Calculated using the 3.82 eV ground state electron affinity measured by J. Berkowitz, W. A. Chupka, and T. A. Walter, J. Chem. Phys. **50**, 1497 (1969).
[33]R. Bersohn, in *Molecular Energy Transfer*, edited by R. Levine and J. Jortner, (Wiley, New York, 1976), pp. 154–161.
[34]D. Feldman, Z. Naturforsch. **259**, 621 (1970).